Neuroradiology
https://doi.org/10.1007/s00234-024-03290-6

DIAGNOSTIC NEURORADIOLOGY

# Atrophy of the cholinergic regions advances from early to late mild cognitive impairment

Ying-Liang Larry Lai[1] · Fei-Ting Hsu[2] · Shu-Yi Yeh[3] · Yu-Tzu Kuo[3] · Hui-Hsien Lin[4] · Yi-Chun Lin[3] · Li-Wei Kuo[5,6] · Cheng-Yu Chen[7,8] · Hua-Shan Liu[3,9] · for the Alzheimer's Disease Neuroimaging Initiative

Received: 18 August 2023 / Accepted: 10 January 2024


## Abstract

**Purpose** We investigated the volumetric changes in the components of the cholinergic pathway for patients with early mild cognitive impairment (EMCI) and those with late mild cognitive impairment (LMCI). The effect of patients' apolipoprotein 4 (APOE-ε4) allele status on the structural changes were analyzed.

**Methods** Structural magnetic resonance imaging data were collected. Patients' demographic information, plasma data, and validated global cognitive composite scores were included. Relevant features were extracted for constructing machine learning models to differentiate between EMCI (n = 312) and LMCI (n = 541) and predict patients' neurocognitive function. The data were analyzed primarily through one-way analysis of variance and two-way analysis of covariance.

**Results** Considerable differences were observed in cholinergic structural changes between patients with EMCI and LMCI. Cholinergic atrophy was more prominent in the LMCI cohort than in the EMCI cohort ($P < 0.05$ family-wise error corrected). APOE-ε4 differentially affected cholinergic atrophy in the LMCI and EMCI cohorts. For LMCI cohort, APOE-ε4 carriers exhibited increased brain atrophy (left amygdala: $P = 0.001$; right amygdala: $P = 0.006$, and right Ch123, $P = 0.032$). EMCI and LCMI patients showed distinctive associations of gray matter volumes in cholinergic regions with executive ($R^2 = 0.063$ and 0.030 for EMCI and LMCI, respectively) and language ($R^2 = 0.095$ and 0.042 for EMCI and LMCI, respectively) function.

**Conclusions** Our data confirmed significant cholinergic atrophy differences between early and late stages of mild cognitive impairment. The impact of the APOE-ε4 allele on cholinergic atrophy varied between the LMCI and EMCI groups.

**Keywords** Early mild cognitive impairment (EMCI) · mild cognitive impairment (MCI) · cholinergic pathway · nucleus basalis of Meynert · APOE-ε4 allele

## Introduction

Alzheimer's disease (AD), a progressive neurodegenerative disease, has a long preclinical phase involving the progressive accumulation of pathological changes in the brain [1].

Mild cognitive impairment (MCI), which is a potential sign of severe cognitive decline, is regarded as a transitional stage between normal cognitive aging and AD. MCI is defined as a decline in cognitive ability, leading to objective cognitive impairments and subjective complaints, with maintenance of the ability to perform daily activities [2]. The Alzheimer's Disease Neuroimaging Initiative (ADNI) is a large-scale observational study of normal aging, MCI, and AD. According to Wechsler Memory Scale-Revised Logical Memory II scores, MCI can be classified into 2 subtypes, early MCI (EMCI) and late MCI (LMCI) [3–5]. Compared with LMCI, EMCI is associated with a reduced risk of progression to dementia or AD [6, 7]. Furthermore, EMCI has more heterogeneous characteristics than LMCI [8]. Earlier findings indicated higher proportions of EMCI patients who exhibited levels of cerebrospinal fluid (CSF) and cortical thickness similar to those observed in cognitively normal

Cheng-Yu Chen and Hua-Shan Liu who contributed equally to this work.

Data used in preparation of this article were obtained from the Alzheimer's Disease Neuroimaging Initiative (ADNI) database (adni.loni.usc.edu). As such, the investigators within the ADNI contributed to the design and implementation of ADNI and/or provided data but did not participate in analysis or writing of this report. A complete listing of ADNI investigators can be found at: http://adni.loni.usc.edu/wp-content/uploads/how_to_apply/ADNI_Acknowledgement_List.pdf.

Extended author information available on the last page of the article

Published online: 19 January 2024

subjects [8]. EMCI potentially indicates an early point in the clinical spectrum, whereas LMCI likely indicates a later point (progression to AD) [9]. Early interventions against EMCI may ensure timely treatment and delay progression to AD, which involves irreversible brain damage [10]. Therefore, sensitive biomarkers for distinguishing between EMCI and LMCI characteristics are urgently needed.

The cholinergic pathway in the basal forebrain (BF), which is essential for utilizing the neurotransmitter acetylcholine, comprises dense cholinergic neuron clusters, particularly in cholinergic nuclei 1, 2, and 3 (Ch123), and the nucleus basalis of Meynert (NBM, i.e., Ch4) [11]. Ch1/Ch2 predominantly project their axons to the hippocampus, playing a crucial role in modulating hippocampal functions related to memory formation and retrieval [8]. Ch3 primarily provides innervation to the olfactory bulb, potentially influencing olfactory memory and sensory processing [6, 8]. Ch4 projects to the neocortex and sends cholinergic fibers to the amygdala, thereby influencing both cognitive and emotional processes. The selective vulnerability of the cholinergic pathway to AD has been reported. Cholinergic deficiency is associated with the formation of amyloid-beta (Aβ) plaques, development of taupathy, and severity of AD [12]. MCI leads to a reduction in the number of cholinergic basal forebrain (BF) neurons; this condition is characterized by the hyperphosphorylation of Tau and the formation of neurofibrillary tangles within BF neurons [11, 13–15]. Neuroimaging findings have revealed that normal older adults with abnormal CSF levels have higher longitudinal cholinergic degeneration than their healthy counterparts [16]. Cholinergic volume atrophy can predict the long-term degeneration of the entorhinal cortex, which is a major target of cholinergic innervation and neurocognitive decline [17, 18].

The APOE gene, with its three main isoforms ε2, ε3, and ε4, plays a crucial role in Alzheimer's disease by influencing the aggregation and clearance of amyloid-beta (Aβ) in the brain [19, 20]. The ε2 isoforms generally exhibit protective effects against AD, enhancing Aβ clearance due to their higher affinity for lipid particles and effective binding with Aβ [20]. The ε3 isoform is considered neutral in AD risk, providing a balanced Aβ binding and clearance capability. In contrast, the ε4 isoforms are less effective at binding Aβ, resulting in decreased clearance and increased Aβ aggregation in the brain [20]. A proposed mechanism suggests that APOE-ε4 augments the interaction between Aβ and specific neuronal receptors, such as α7 nicotinic acetylcholine receptors. This can facilitate the uptake of the Aβ-α7 receptor complex into neurons, potentially leading to Aβ aggregation, believed to be precursors of amyloid plaques in the cerebral cortex [21–24]. Although it has been shown that APOE-ε4 is associated with cholinergic compensatory mechanisms [25], few studies have focused on the effect of APOE-ε4 on the cholinergic pathway in patients with EMCI and LMCI.

This study analyzed the volumetric changes in the cholinergic regions for EMCI and LMCI patients. We hypothesized that the effect of APOE-ε4 would make these changes distinct between the two groups. By integrating cholinergic structural data, composite neurocognitive scores, and plasma biomarkers, we employed a machine learning (ML) model to differentiate between EMCI and LMCI patients and predict their neurocognitive function.

## Materials and Methods

### Subjects

Data used in this study were obtained from the ADNI database (https://adni.loni.usc.edu) [26]. The ADNI was launched in 2003, representing a partnership between public and private entities. This initiative was led by Michael W. Weiner (MD; principal investigator). The primary goal of the ADNI study was to investigate whether serial magnetic resonance imaging (MRI), positron emission tomography, other biological markers, and clinical and neuropsychological assessment can be combined to assess the progression of MCI and early AD. For the present study, MRI data were downloaded from the ADNI-1, ADNI1/Go, ADNI-2, and ADNI-3 databases; in addition, patients' demographic information, neurocognitive data, and validated composite scores derived from baseline global cognitive composite scores were collected. This study was approved by the ethics committees of all participating institutions. Written informed consent was obtained from all participants. ADNI global cognitive composite scores, including memory (MEM), executive functioning (EF), language (LAN), and visuospatial functioning (VS), along with Aβ 1 to 42 (Aβ42), total tau (Tau), and Tau phosphorylated at threonine 181 (pTau) at baseline have been described in detail in previous studies [27, 28]. This study included patients whose imaging data passed our image quality control assessment. Thus, 312 patients with EMCI and 541 patients with LMCI were included in this study. Subsequently, the included patients were classified according to their APOE-ε4 allele carrier status. The steps of APOE-4 genotyping are detailed here: http://www.adni-info.org.

### MRI Data

High-resolution T1 structural MRI data, obtained using 1.5 T and 3 T MRI scanners, were downloaded, and summary are presented in Supplementary Table S1 (Summary of 3D T1-weighted MRI protocols in ADNI-1, ADNI-Go, ADNI-2, and ADNI-3). The detailed MRI protocols are available on the ADNI website (http://adni.loni.usc.edu/methods/documents/mri-protocols/).

## Data Analyses

Region-of-interest (ROI) masks were created using the SPM Anatomy Toolbox [29] and cytoarchitectonic probability anatomical maps [30, 31]. The bilateral Ch123; NBM; and amygdala were included in the ROI masks, as depicted in Fig. 1a. The CAT12 toolbox was used to perform voxel-based morphometry (VBM) analyses [32, 33]. Preprocessing included complete and iterative bias correction in statistical parametric mapping; normalization to the standard template of Montreal Neurological Institute by using a diffeomorphic anatomical registration algorithm; and segmentation into gray matter (GM), white matter (WM), and CSF. A Gaussian filter was used to smooth the normalized GM images (4-mm full-width half-maximum). Quality control was performed to eliminate potential outliers. Before analyses, image quality was evaluated by using the toolbox of Check Sample Homogeneity from CAT12 for VBM data [34]. All data were quality-controlled in accordance with the CAT12 procedures. Data with inhomogeneity, images with low signal intensity, and data with warping errors were excluded. After the correlations between all volumes were calculated, data with correlation coefficient values of less than two standard deviations were omitted from the analysis [34].

## Statistical Analyses

Between-group differences in demographic characteristics were assessed using one-way analysis of variance and chi-square tests for categorical variables. After adjustment for age, sex, educational level, and total intracranial volume (TIV; this comprises GM, WM, and CSF), two-way analysis of covariance (ANCOVA) was performed to examine the main effects of group (EMCI vs LMCI) and APOE-ε4 and the interaction effect of group × APOE-ε4 on the global composite scores.

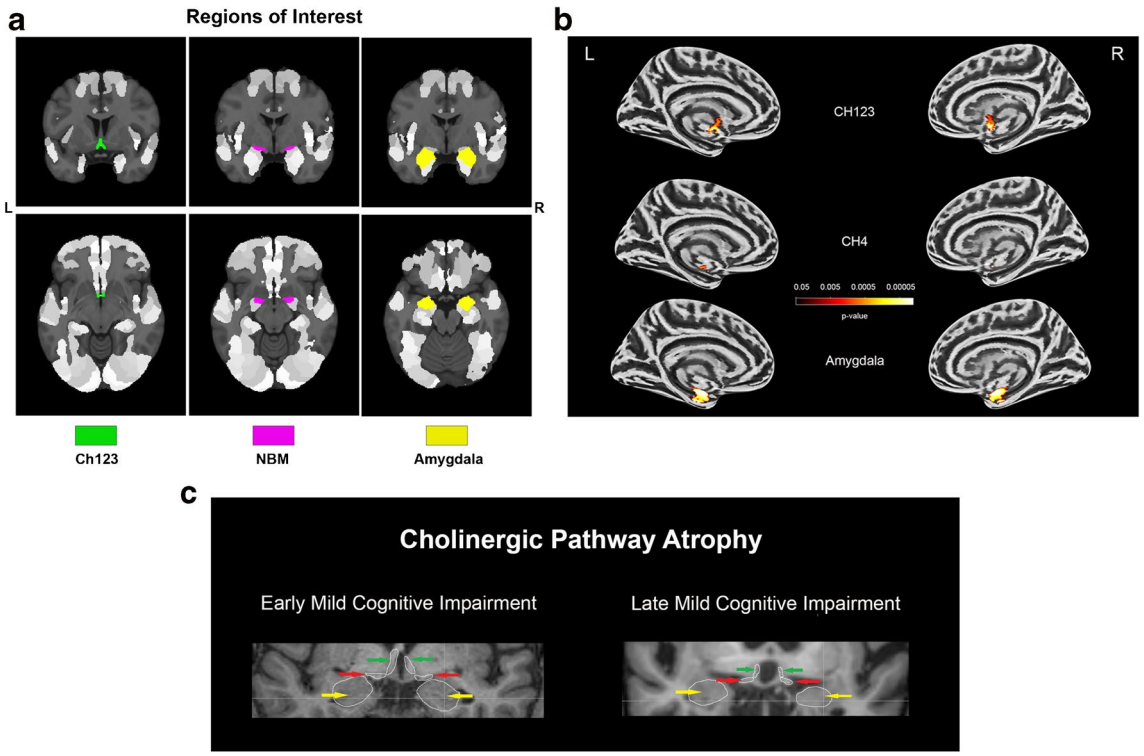


**Fig. 1** **a** Masks for regions of interest (ROIs) of the bilateral CH123; CH4; and amygdala. **b** Main effect of group differences on amygdala and basal forebrain subregion volume through voxel-based morphometry 2 × 2 ANCOVA (two groups × APOE-ε4 carrier status) analysis. Significant atrophy of gray matter volume is presented on the inflated cortical surfaces ($P < 0.05$ family-wise error corrected). **c** A comparison of cholinergic atrophy between representative subjects from the EMCI and LMCI groups. For EMCI, a 79.5-year-old female non-APOE-ε4 carrier exhibited volumes of the left amygdala = 1662.5 $mm^3$, right amygdala = 1439.9 $mm^3$, left NBM = 67.8 $mm^3$, right NBM = 48.5 $mm^3$, left CH123 = 94.1 $mm^3$, and right CH123 = 79.5 $mm^3$, as indicated by yellow, red, and green arrows for amygdala, NBM, and CH123, respectively. For LMCI, a 79.3-year-old female APOE-ε4 carrier subject showed volumes of the left amygdala = 1218.1 $mm^3$, right amygdala = 1065.2 $mm^3$, left NBM = 53.4 $mm^3$, right NBM = 38.2 $mm^3$, left CH123 = 70.1 $mm^3$, and right CH123 = 65.0 $mm^3$, as indicated by yellow, red, and green arrows for amygdala, NBM, and CH123, respectively. **d** Significant atrophy in both basal forebrain and amygdala volume (in cubic millimeters) for EMCI and LMCI. *$P < 0.05$. EMCI: early cognitive impairment, LMCI: late cognitive impairment, CH123: cholinergic nuclei 1, 2, and 3, CH4: nucleus basalis of Meynert, Amy: amygdala, R: right side, L: left side, ANCOVA: analysis of covariance

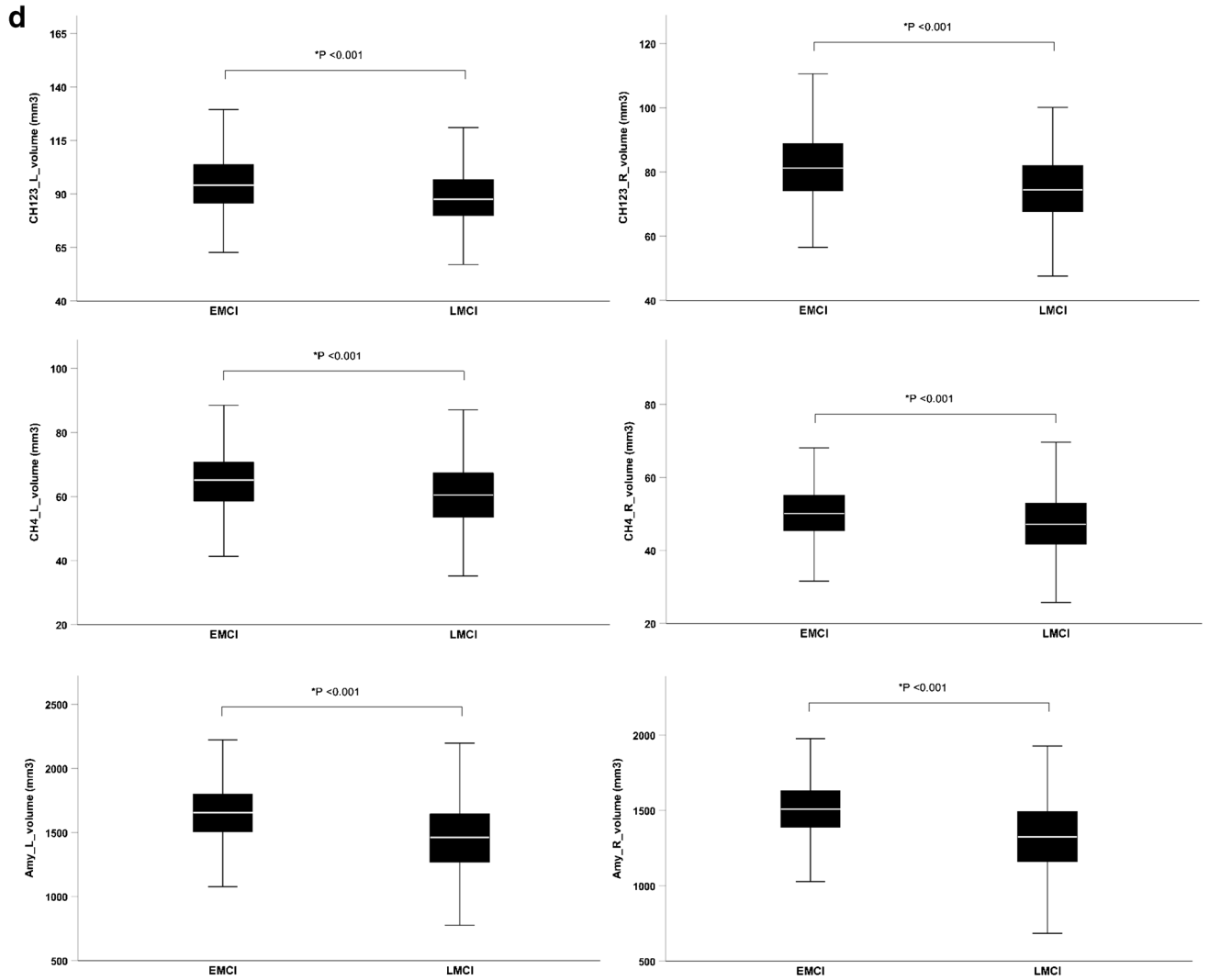


**Fig. 1** (continued)

SPSS (version 27.0) was used for statistical analyses. The significance level was set at $P < 0.05$.

## Between-Group Comparison of Volumetric Measurements

The data were modeled through 2 × 2 ANCOVA to compare volumetric measurements between the groups and to evaluate the APOE-ε4 effect; thus, the following design cells were created: EMCI (+), EMCI (−), LMCI (+), and LMCI (−); the (+) sign denotes APOE-ε4 carriers, and the (−) sign denotes noncarriers. Age, sex, educational level, and TIV were all included as nuisance covariates. We analyzed the main effects of group (EMCI vs LMCI) and APOE-ε4 (carriers vs noncarriers) and the interaction effect of group × APOE-ε4. To correct for multiple comparisons, the nonparametric threshold-free cluster enhancement method was used with 10 000 permutations [35, 36]. Statistical significance was set at $P < 0.05$ when using the family-wise error method. SPM software was used for analysis. The MarsBaR toolbox (http://marsbar.sourceforge.net) was used to extract mean values for the significant clusters identified in ANCOVA.

## Associations between Volumetric Changes in the Cholinergic Regions and Neurocognitive Performance

To investigate the effect of different group on the relationship between the cholinergic volume atrophy and cognitive performance, we compared the correlation coefficients between EMCI and LMCI by analyzing the interaction effects (i.e.,

**Table 1** Demographic characteristics of two different subject groups

| | | EMCI (n = 312) | LMCI (n = 541) | F or $\chi^2$ (P value) |
|---|---|---|---|---|
| Age | Mean ± SD | 71.04 ± 7.35 | 73.83 ± 7.59 | **0.001*** |
| Sex | M/F | 171/141 | 329/212 | 0.09 |
| Education (years) | Mean ± SD | 16.11 ± 2.67 | 15.92 ± 2.83 | 0.34 |
| TIV | Mean ± SD | 1469.02 ± 152.09 | 1478.67 ± 155.38 | 0.38 |

EMCI: early mild cognitive impairment, LMCI: late mild cognitive impairment. *$P < 0.05$

*group* × NBM_L, *group* × NBM_R, *group* × amygdala_L and *group* × amygdala_R) of the following linear regression:

neurocognitive scores = NBM_L + NBM_R + amygdala_L + amygdala_R + *group* + (*group* × NBM_L) + (*group* × NBM_R) + (*group* × amygdala_L) + (*group* × amygdala_R) + age + sex + edu + TIV.

As shown above, the neurocognitive scores (MEM, EF, LAN or VS) were considered as the dependent variable, whereas the volume measurements in bilateral NBMs and amygdalae, *group (EMCI vs. LMCI)*, interaction terms between the *group effect* and volume measurements in each ROI were treated as the independent variables. Age, sex, edu, and TIV were added as the independent variables. The interaction term between *group* and VBM measurements was used to test the hypothesis that the relationship between neurocognitive performance and volumetric changes in the NBM and the amygdala is different between the EMCI and LMCI groups. All the statistical results are reported at the $P < 0.05$ significance level.

## ML Analysis

### Support Vector Machine Analysis

To classify patients with LMCI and those with EMCI, we used the ML algorithm of a nonlinear support vector machine (SVM) with a radial basis function kernel to analyze brain atrophy and neurocognitive features [37, 38]. By constructing a hyperplane with the highest between-class margin, SVM divides a data set into two classes [39]. The most accurate gamma and overfitting constant C parameters were obtained using the tenfold cross-validation method [40–42]. The data were randomly divided into training and test data sets (ratio: 7:3 [training:test]). The accuracy, sensitivity, and specificity values were calculated. Classification was conducted based on the following features: bilateral volumes of Ch123, Ch4, and the amygdala; TIV; APOE-ε4 status; demographic data, such as age, sex, and educational level; memory; EF; language; VS; and Aβ42 level; Tau level; and pTau level. The data were converted into z-scores. The area under the receiver-operating characteristic curve (AUC) values of the classification models were calculated to evaluate classifier performance. *DeLong test* was used to evaluate the difference of AUC between classification models using different sets of combined features [43].

### Support Vector Regression

Support vector regression (SVR) analysis was performed to identify the best predictors of memory and EF. The tenfold cross-validation method was used. We compared the predictive performance of the SVR model with different predictors of volumetric measurement and plasma biomarker features. Root mean squared error (RMSE) values were determined to compare the results obtained using different feature combinations.

**Table 2** Comparison between APOE-ε4 allele carriers and non-carriers in cognitive performance for each subject group

| Group | Cognitive performances | APOE ε4 status | Mean (std) | P-value |
|---|---|---|---|---|
| EMCI | MEM | APOE ε4 (-) | 0.666 (0.591) | **0.016*** |
| | | APOE ε4 (+) | 0.506 (0.554) | |
| | EF | APOE ε4 (-) | 0.652 (0.782) | **0.032*** |
| | | APOE ε4 (+) | 0.450 (0.864) | |
| | LAN | APOE ε4 (-) | 0.531 (0.718) | 0.476 |
| | | APOE ε4 (+) | 0.471 (0.748) | |
| | VS | APOE ε4 (-) | 0.140 (0.693) | 0.320 |
| | | APOE ε4 (+) | 0.063 (0.640) | |
| LMCI | MEM | APOE ε4 (-) | 0.078 (0.589) | **0.001*** |
| | | APOE ε4 (+) | -0.174 (0556) | |
| | EF | APOE ε4 (-) | 0.119 (0.865) | 0.193 |
| | | APOE ε4 (+) | 0.024 (0.827) | |
| | LAN | APOE ε4 (-) | 0.073 (0.739) | 0.242 |
| | | APOE ε4 (+) | -0.004 (0.797) | |
| | VS | APOE ε4 (-) | -0.089 (0.769) | 0.220 |
| | | APOE ε4 (+) | -0.171 (0.777) | |

APOE-ε4 (+): APOE-ε4 carriers, APOE-ε4 (–): non-APOE-ε4 carriers, EMCI: early mild cognitive impairment, LMCI: late mild cognitive impairment, MEM: memory function, EF: executive function, LAN: language function, VS: visuospatial function

*$P < 0.05$

## Results

### Demographics and Neurocognitive Data

The demographic and statistical characteristics of the EMCI and LMCI groups are summarized in Table 1. No significant between-group difference was found in sex, educational level, or TIV. The patients in the EMCI group was significantly younger than the patients in the LMCI group. Hence, all subsequent analyses were performed using age as a covariate. Two-way analysis of variance analysis of the patients' neurocognitive scores revealed the significant main effects of group on MEM ($F=207.30$; $P<0.0005$), EF ($F=43.02$; $P<0.0005$), LAN ($F=54.77$; $P<0.0005$), and VS ($F=15.99$; $P<0.0005$). MEM, EF, LAN, and VS were significantly lower in patients with LMCI than in those with EMCI. Furthermore, significant main effects of APOE-ε4 were observed on MEM ($F=34.31$; $P<0.0005$) and EF ($F=12.83$; $P<0.0005$), but not on LAN or VS. Table 2 presents the neurocognitive data of APOE-ε4 carriers and noncarriers in the EMCI and LMCI groups. Among patients with EMCI, the APOE-ε4 allele carrier status affected MEM and EF. Among patients with LMCI, the APOE-ε4 allele carrier status affected MEM. However, no interaction effect of group × APOE-ε4 was observed on any of the neurocognitive parameters.

### VBM Group Comparison Through ANCOVA

Significant main effects of group were observed in the bilateral amygdala (left: $P=0.001$; right: $P=0$ 0.001) and BF subregion (left Ch123: $P=0.001$; right Ch123: $P=0.001$; left NBM: $P=0.001$; right NBM: $P=0$ 0.001, Fig. 1b; Supplementary Table S2). Figure 1c depicts the comparison of cholinergic atrophy between representative subjects from the EMCI and LMCI groups. Post hoc tests revealed that the LMCI group had significantly more brain atrophy in the Ch123 and NBM/amygdala pathway than did the EMCI group (Fig. 1d).

Significant main effects of APOE-ε4 were observed in the bilateral amygdala (left: $P=0.001$; right: $P=0.001$) and BF subregion (left Ch123: $P=0.0044$; right Ch123: $P=0.034$; left NBM: $P=0.001$; right NBM: $P=0.001$; Fig. 2; Supplementary Table S3). Table 3 presents a comparison of APOE-ε4 carriers and noncarriers in each group. In the LMCI group, the volumetric reductions in the bilateral NBM and amygdala were significantly larger in APOE-ε4 carriers than in noncarriers. Significant interaction effects of group × APOE-ε4 were observed in the bilateral amygdala (left: $P=0.001$; right: $P=0.006$) and right BF Ch123 subregion ($P=0.032$). In the LMCI group, APOE-ε4 carriers had significantly more brain atrophy than did noncarriers. However, there is no difference of volumetric changes between APOE-ε4 carriers and noncarriers in the EMCI group (Fig. 3; Supplementary Table S4). Our findings revealed significant between-group differences in the effect of APOE-ε4 on the volumetric loss of the amygdala and BF subregion in the cholinergic system.

The ANCOVA results of between-group comparisons of the number of APOE-ε4 alleles are presented in Supplementary Tables S5. We found significant group effects of the number of APOE-ε4 alleles on memory, EF, and bilateral NBM volumetric measurements in the EMCI group. In the

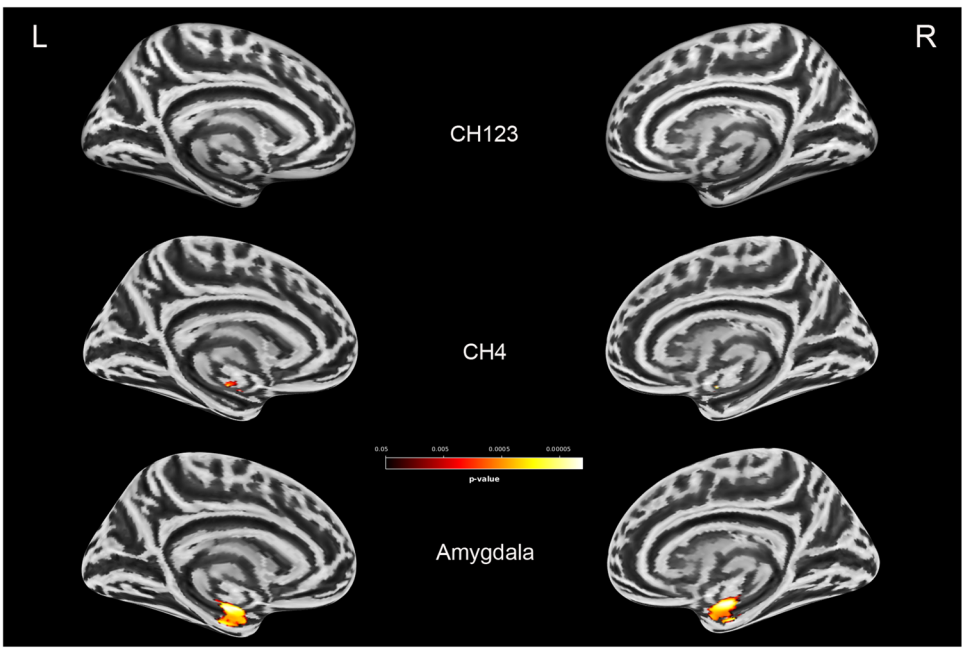


**Fig. 2** Main effect of APOE-ε4 on amygdala and basal forebrain subregion volume through voxel-based morphometry 2 × 2 ANCOVA (two groups × APOE-ε4 carrier status) analysis. Significant atrophy of gray matter volume is presented on the inflated cortical surfaces ($P<0.05$ family-wise error corrected). CH123: cholinergic nuclei 1, 2, and 3, CH4: nucleus basalis of Meynert, Amy: amygdala, R: right side, L: left side, ANCOVA: analysis of covariance

**Table 3** Volumetric comparison between APOE-ε4 allele carriers (+) and non-carriers (–)

| | | EMCI | LMCI |
|---|---|---|---|
| CH123_L | APOE-ε4 + | 95.94 ± 12.23 | 88.45 ± 12.53 |
| | APOE-ε4- | 94.57 ± 13.91 | 88.63 ± 12.57 |
| | P-value | 0.367 | 0.863 |
| CH123_R | APOE-ε4 + | 82.26 ± 10.12 | 74.63 ± 10.52 |
| | APOE-ε4- | 80.86 ± 11.23 | 75.22 ± 10.06 |
| | P-value | 0.257 | 0.508 |
| NBM_L | APOE-ε4 + | 64.12 ± 9.20 | 58.96 ± 10.01 |
| | APOE-ε4- | 65.04 ± 9.30 | 62.35 ± 9.81 |
| | P-value | 0.388 | **0.001*** |
| NBM_R | APOE-ε4 + | 49.79 ± 7.54 | 46.05 ± 7.90 |
| | APOE-ε4- | 50.59 ± 7.21 | 48.64 ± 8.24 |
| | P-value | 0.351 | **0.001*** |
| Amy_L | APOE-ε4 + | 1647.65 ± 223.31 | 1407.64 ± 256.69 |
| | APOE-ε4- | 1637.19 ± 243.42 | 1509.90 ± 269.61 |
| | P-value | 0.699 | **0.001*** |
| Amy_R | APOE-ε4 + | 1504.31 ± 204.25 | 1282.64 ± 223.86 |
| | APOE-ε4- | 1499.94 ± 202.67 | 1371.79 ± 246.66 |
| | P-value | 0.852 | **0.001*** |

Data are presented in unit of cubic millimeter of mean volume ± standard deviation adjusted for age, sex, edu, and total intracranial volume. NBM: nucleus basalis of Meynert, Amy: amygdala, EMCI: early mild cognitive impairment, LMCI: late mild cognitive impairment, R: right side, L: left side. *$P < 0.05$

LMCI group, we found significant group effects of the number of APOE-ε4 alleles on memory and bilateral NBM and amygdala volumetric measurements. Post hoc tests revealed significant differences of the left NBM and bilateral amygdala volumetric measurements between the homozygous (ε4-ε4) and heterozygous (ε3-ε4) carriers of APOE-ε4 in the LMCI group (Supplementary Table S5c), but not in the EMCI group (Supplementary Table S5d).

### Correlation between VBM and neurocognitive measurements

For the association between cholinergic volumetric changes and cognitive performance, we observed significant interaction effects of group × left amygdala measurements in modulating the neurocognitive performance of EF and LAN (Fig. 4 and Supplement Table S6). For both EF and LAN, EMCI ($R^2 = 0.063$ and 0.095 for EF and LAN, respectively) group exhibited significantly stronger correlations between left amygdala and neurocognitive performance than LMCI ($R^2 = 0.030$ and 0.042 for EF and LAN, respectively) subjects ($P = 0.035$ and $P = 0.043$ for EF and LAN, respectively).

### ML Analysis Results

#### SVM Results

The results of ML-based classification were presented in the Fig. 5 and Table 4. The incorporation of only plasma biomarkers (Aβ42 + Tau + pTau) showed the lowest accuracy (accuracy = 0.68; AUC = 0.67, respectively). The combination of the plasma biomarkers with neurocognitive function (MEM and EF) and the VBM features of Ch4 + amygdala provided the highest accuracy (0.81) and AUC (0.83), followed by the combination of classifiers with VBM and neurocognitive features (i.e., NBM + Amy + MEM + EF, accuracy = 0.79 and AUC = 0.80).

Supplementary Table S7 presents the classification results for all features (All) and feature subsets excluding APOE-ε4 status (All-APOE-ε4). A feature was considered to be important if the resultant accuracy score decreased when the feature was removed from the classification process[44]. The removal of APOE-ε4 improved the classification accuracy. Therefore, APOE-ε4 status was not included in the final ML classification model.

#### SVR Results

SVR results are presented in Table 5. The best predictive performance for global composite memory scores was exhibited by a model constructed by combining VBM (NBM + amygdala) parameters and the plasma biomarkers of Aβ42, Tau, and pTau (RMSE = 0.54). Similar to memory function, the best predictive performance for global EF scores was exhibited by a model constructed by combining VBM (NBM + amygdala) parameters with the plasma biomarkers of Aβ42, Tau, and pTau (RMSE = 0.78). The results of predicted values generated by SVR was shown in Fig. 6.

## Discussion

### Major Findings

Significant differences in atrophy of regions within the cholinergic pathway were observed between EMCI and LMCI patients. The LMCI group exhibited significantly more cholinergic atrophy than did the EMCI group. Our

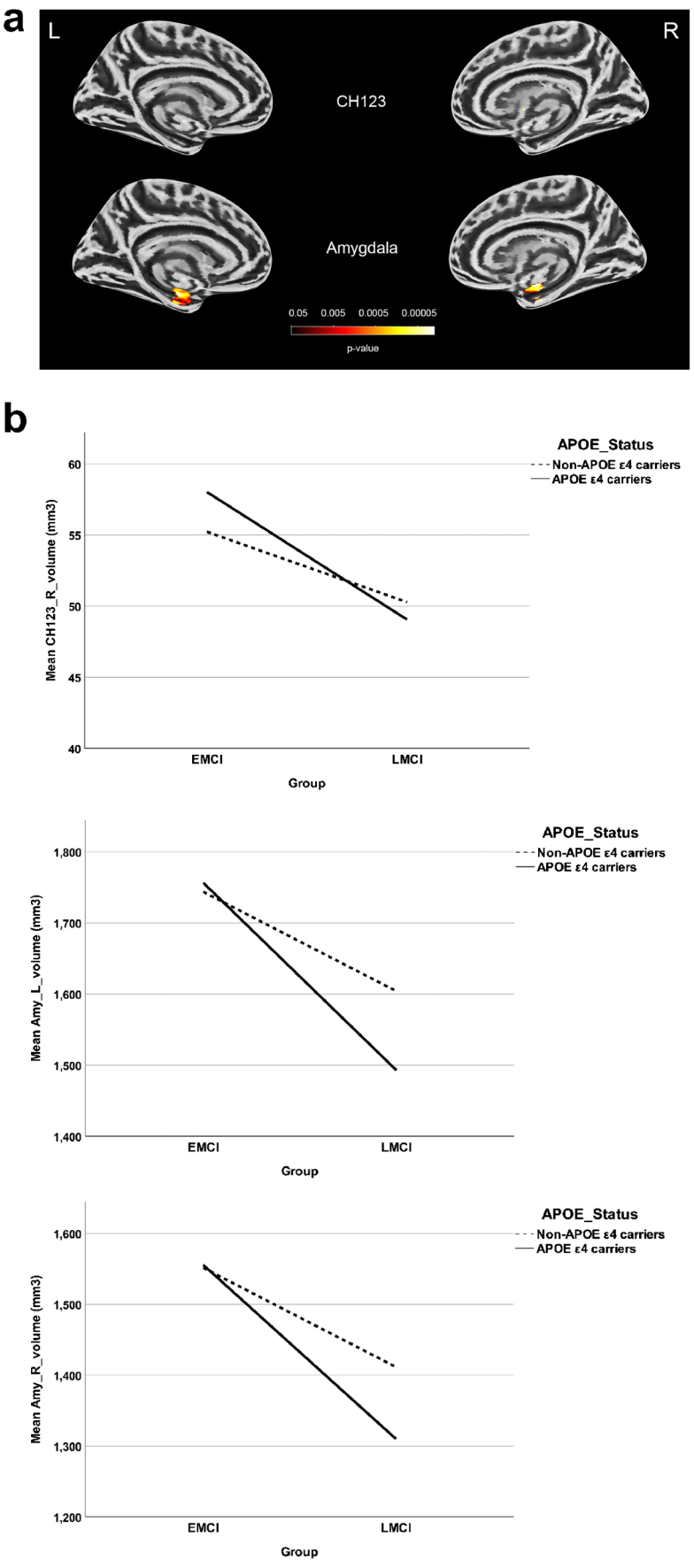


**Fig. 3** **a** Interaction effect of group × APOE-ε4 on amygdala and basal forebrain subregion volume through voxel-based morphometry 2 × 2 ANCOVA (two groups × APOE-ε4 carrier status) analysis. Significant atrophy of gray matter volume is presented on the inflated cortical surfaces ($P < 0.05$ family-wise error corrected). **b** The significant interaction effect of group × APOE-ε4 on bilateral amygdala and right CH123 subregion mean volume (in cubic millimeter) for patients with LMCI as compared with EMCI subjects. APOE-ε4 carriers exhibited more volume reduction than non-carriers in the LMCI group. EMCI: early cognitive impairment, LMCI: late cognitive impairment, CH123: cholinergic nuclei 1, 2, and 3, Amy: amygdala, R: right side, L: left side, ANCOVA: analysis of covariance

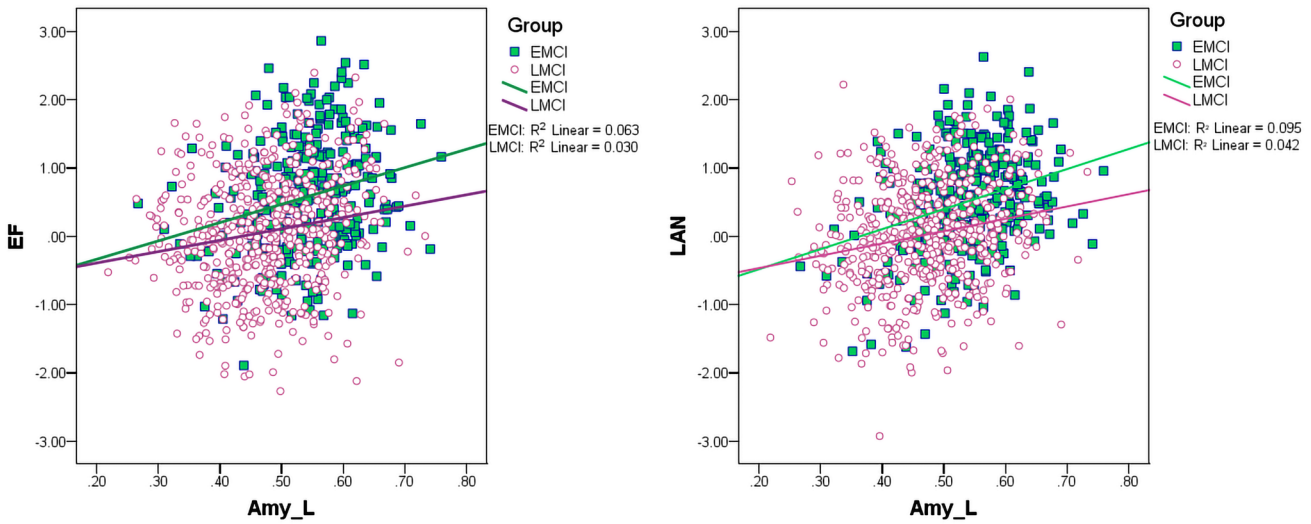


**Fig. 4** Plots of the associations between volumetric and neurocognitive measurements using the regression model: neurocognitive scores = NBM_L + NBM_R + amygdala_L + amygdala_R + *group* + (*group* × NBM_L) + (*group* × NBM_R) + (*group* × amygdala_L) + (*group* × amygdala_R) + age + sex + edu + TIV. Different slopes of the regression lines indicated the interaction effect of group by cholinergic volume in neurocognitive performance. EMCI group showed stronger correlations between cholinergic volume in the left amygdala and neurocognitive performance of EF and LAN than LMCI subjects. Amy_L: left amygdala, EF: executive function, LAN: language function, EMCI: early mild cognitive impairment, LMCI: late mild cognitive impairment. Data are presented in normalized volume. $R^2$: square of the correlation

findings also indicated that the APOE-ε4 allele differentially affected cholinergic atrophy between the LMCI and EMCI groups. In the LMCI group, APOE-ε4 carriers had more GM atrophy than did noncarriers; by contrast, in the EMCI group, no difference in volumetric changes was noted between APOE-ε4 carriers and noncarriers (Fig. 3 and Table 3). Our results further demonstrated the different associations of the cholinergic volume and neurocognitive performance between EMCI and LMCI. EMCI group showed a stronger correlation between the cholinergic volume and neurocognitive performance than LMCI group. We then constructed an ML model by incorporating features related to the cholinergic structure, plasma biomarkers, and neurocognitive parameters. For SVM classification, the combination of the features of NBM, amygdala, memory, Aβ42 level, Tau and pTau levels exhibited the highest accuracy (81%) and AUC (0.83), as shown in Table 4. By employing the combined features of cholinergic volume and plasma biomarkers, the ML-based predictive model for SVR further exhibited a high predictive power for the global composite memory and EF scores, confirming that these biomarkers can facilitate the prediction of neurocognitive function in these patients (Fig. 6).

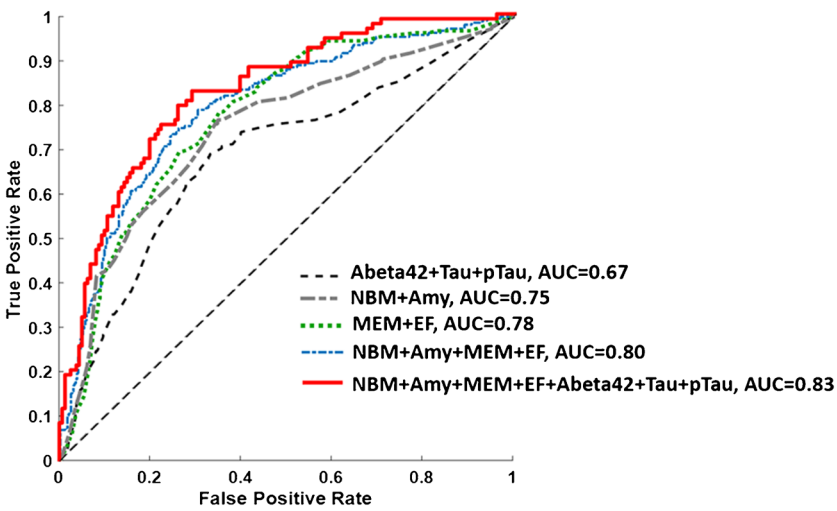


**Fig. 5** Receiver operating characteristic (ROC) curves obtained from classification of LMCI and EMCI. EMCI: early cognitive impairment, LMCI: late cognitive impairment, NBM: nucleus basalis of Meynert, Amy: amygdala, R: right side, L: left side, Abeta42: amyloid-beta 1–42, Tau: total tau, pTau: Tau phosphorylated at threonine 181

**Table 4** Machine learning classification outcomes for classifying LMCI and EMCI groups

| | AUC | ACC | Sen | Spec | P-value |
|---|---|---|---|---|---|
| Abeta42 + Tau + pTau | 0.67 | 0.68 | 0.82 | 0.36 | **$< 10^{-6}$*** |
| NBM + Amy | 0.75 | 0.73 | 0.79 | 0.65 | **0.002*** |
| MEM + EF | 0.78 | 0.75 | 0.75 | 0.72 | **0.04*** |
| NBM + Amy + MEM + EF | 0.80 | 0.79 | 0.77 | 0.75 | 0.21 |
| NBM + Amy + MEM + EF + Abeta42 + Tau + pTau | **0.83** | **0.81** | **0.85** | **0.78** | – |

AUC: area under the curve of ROC, Acc: accuracy, Sens: sensitivity, Spec: specificity, EMCI: early mild cognitive impairment, LMC: late mild cognitive impairment, NBM: nucleus basalis of Meynert, Amy: amygdala, Abeta42: amyloid-beta 1–42, Tau: total tau, pTau: Tau phosphorylated at threonine 181. P-value represents the comparison of performance with results generated by the features of NBM + Amy + MEM + EF + Abeta42 + Tau + pTau. *$P < 0.05$

**Table 5** Root mean square error (RMSE) values for the support-vector regression model in predicting memory (MEM) and effective (EF) function across all subject groups using different sets of combined features

| | RMSE | |
|---|---|---|
| | MEM | EF |
| Abeta42 + Tau + pTau | 0.65 | 0.87 |
| NBM + Amy | 0.60 | 0.81 |
| NBM + Amy + Abeta42 + Tau + pTau | 0.54 | 0.78 |

## VBM

### Main Effect of Group

The observation of greater GM atrophy in regions of the cholinergic pathway among patients with LMCI than EMCI suggests that structural changes in the cholinergic pathway could potentially serve as reliable biomarkers for distinguishing between EMCI and LMCI. The differences in these structural changes between EMCI and LMCI corroborate those in a study reporting that the proportion of patients with false-positivity was higher in the EMCI group than in the LCMI group[27]. Patients with EMCI still have relatively normal neurocognitive performance, and the changes in brain MRI images are subtle[27]. Their brains resemble those of the general healthy population.

### Main Effect of APOE-ε4

The effect of APOE-ε4 on the brain atrophy in the cholinergic pathway may involve higher Aβ accumulation, leading to a higher degree of neurodegeneration [45, 46]. In an animal study, Aβ42 was injected into the brains of rats; this led to a considerable reduction in cholinergic function, resulting in abnormal changes in mitochondrial function and integrity [24]. APOE-ε4-mediated accelerated neurocognitive decline was also observed in Aβ-positive normal individuals, but not in Aβ-negative individuals [47]. Excessive Aβ accumulation can damage the mitochondria in the brain, resulting in

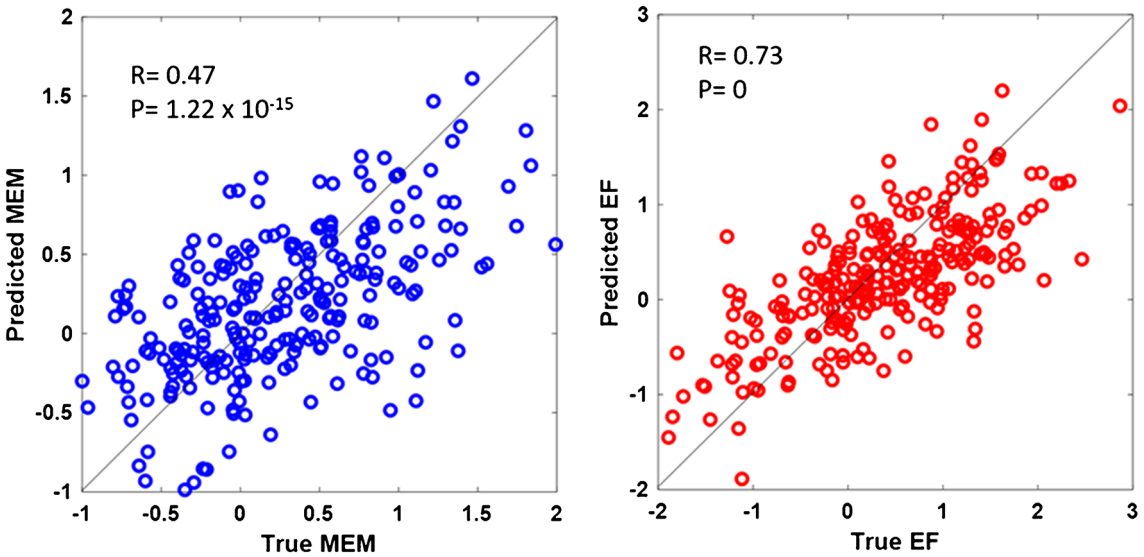


**Fig. 6** Scatter plots of the predicted MEM (R = 0.47, $P = 1.22 \times 10^{-15}$) and EF (R = 0.73, $P = 0$) scores generated by the support vector regression using the combined features of NBM + amygdala + Aβ42 + Tau + pTau for MEM and EF. NBM: nucleus basalis of Meynert, Abeta42: amyloid-beta 1–42, Tau: total tau, pTau: Tau phosphorylated at threonine 181. MEM: memory function. EF: executive function

cognitive dysfunction [23]. Acetylcholine is an excitatory neurotransmitter that is involved in memory performance and other higher-order EFs. By regulating acetylcholine synthesis and release, the central cholinergic nervous system controls acetylcholine levels[48]. In the case of the early loss of BF neurons, the cholinergic control balance in microglia may be disrupted, resulting in the overabundance of proinflammatory activated microglia. This may lead to neuroinflammation because of the reduced cholinergic input to the hippocampus [49].

#### Interaction Effect of Group × APOE-ε4

APOE-ε4 carriers in the LMCI group had more brain atrophy in the cholinergic pathway than did those in the EMCI group (Fig. 3). This finding is consistent with those of studies reporting that the effect of APOE-ε4 on the progression of neurocognitive decline varies across AD stages [50, 51]. APOE-4 carriers with MCI exhibit a slower decline in cognitive ability than those with AD[51]. Our findings revealed that the APOE-ε4-mediated decline in brain function was more prominent in patients with LCMI than in those with EMCI. This finding may be attributed to pTau and Tau levels, which were significantly higher in APOE-ε4 carriers than in noncarriers in the LMCI group [50].

We further evaluated the dose effect of the number of APOE-ε4 alleles on global cognitive composite scores and volumetric changes in the cholinergic pathway in both the EMCI and LMCI groups (Supplementary Table S5). Significant differences in atrophy were observed in the left NBM and bilateral amygdala between homozygous (ε4-ε4) and heterozygous (ε3-ε4) APOE-ε4 carriers in the LMCI group. However, no dose effect of the number of APOE-ε4 alleles was found in the EMCI group; this finding may be attributed to the smaller number of homozygous patients in our EMCI group. The finding in the LMCI group is consistent with that of a study indicating a dose-dependent relationship between APOE-ε4 and AD risk; the risk is higher and the age of onset is younger among homozygous APOE-ε4 carriers than among heterozygotes APOE-ε4 carriers [52]. Approximately 50% of all homozygous APOE-ε4 carriers are likely to develop AD by the age of 85 years; by contrast, this proportion is only 10% among noncarriers [52].

### Association between Cholinergic Atrophy and Neurocognitive Performance

EMCI subjects exhibited a stronger correlation between the left amygdala and neurocognitive performance of EF and LAN than the LMCI subjects (Fig. 4). The correlation between the cholinergic region and neurocognitive performance remarkably distinguished EMCI from LMCI. The weaker correlation between the cholinergic volume and neurocognitive performance in LMCI may be related to a disrupted brain network efficiency in the cholinergic pathway caused by the greater brain atrophy and the impaired cognitive function in this subject group.

### ML Analysis

#### SVM

Machine learning results align with the statistical findings, highlighting significant differences in cholinergic atrophy between the EMCI and LMCI groups. The combined features of cholinergic structural data, plasma biomarkers, and neurocognitive parameters enhances the potential of ML-based classification models for the clinical diagnosis of EMCI and LMCI. In terms of the significance of the given features for the prediction results (Supplementary Table S7), it appears that APOE-ε4 may not have a significant effect on classification outcomes. This assumption is grounded in the observation that the resulting accuracy score does not significantly decrease after excluding the APOE-ε4 feature from the analysis.

#### SVR

The best predictive performance for global composite memory and EF scores was achieved by combining VBM (NBM + amygdala) parameters with Aβ42, Tau, and pTau levels. Similar to the SVM classification results, our findings revealed that the combined features of cholinergic structural data and plasma biomarkers provided high predictive potential for the decline in neurocognitive function in patients with MCI.

## Limitations

Our study has some limitations. Cytoarchitectonic probability anatomical maps [30, 31] were used to define the anatomical ROI for the EMCI and LMCI groups. These MRI volumetric measurements that were used to assess cholinergic pathway degeneration are indirect in nature. Thus, further histopathological analyses are needed to validate our findings. Monitoring individuals from health to the disease state and investigating the structure–function interactions of individual patients may be an effective strategy for predicting neurodegeneration from structural MRI data. Such longitudinal analyses should be performed in future collaborative studies for predicting the early stage of AD. Although the ADNI MRI core facility has established standard protocols (www.adni-info.org), differences

may be present in how MRI imaging data are analyzed because different medical centers use different MRI scanners. Because the ADNI-3 database is still under development, only limited data are available for patients with EMCI and those with LMCI. Despite these limitations, we discovered that models constructed by combining neurocognitive and volumetric measurements and plasma biomarkers can accurately differentiate EMCI from LMCI.

## Conclusions

EMCI and LMCI exhibited different morphometric changes in the cholinergic system of the brain. An increased loss of cholinergic neurons in APOE-ε4 carriers can serve as a biomarker for the differential diagnosis of EMCI from LMCI. Through VBM, we extracted features associated with EMCI/LMCI-related changes in the cholinergic structure. Combined with global composite memory scores, and plasma biomarkers, these features can be successfully incorporated into ML models to differentiate between EMCI and LMCI and predict the neurocognitive functions.

**Supplementary Information** The online version contains supplementary material available at https://doi.org/10.1007/s00234-024-03290-6.

**Acknowledgements** Data collection and sharing for this project was funded by the Alzheimer's Disease Neuroimaging Initiative (ADNI) (National Institutes of Health Grant U01 AG024904) and DOD ADNI (Department of Defense award number W81XWH-12-2-0012). ADNI was funded by the National Institute on Aging, the National Institute of Biomedical Imaging and Bioengineering, and through generous contributions from the following: AbbVie, Alzheimer's Association; Alzheimer's Drug Discovery Foundation; Araclon Biotech; BioClinica, Inc.; Biogen; Bristol-Myers Squibb Company; CereSpir, Inc.; Cogstate; Eisai Inc.; Elan Pharmaceuticals, Inc.; Eli Lilly and Company; EuroImmun; F. Hoffmann-La Roche Ltd. and its affiliated company Genentech, Inc.; Fujirebio; GE Healthcare; IXICO Ltd.; Janssen Alzheimer Immunotherapy Research & Development, LLC.; Johnson & Johnson Pharmaceutical Research & Development LLC.; Lumosity; Lundbeck; Merck & Co., Inc.; Meso Scale Diagnostics, LLC.; NeuroRx Research; Neurotrack Technologies; Novartis Pharmaceuticals Corporation; Pfizer Inc.; Piramal Imaging; Servier; Takeda Pharmaceutical Company; and Transition Therapeutics. This Canadian Institutes of Health Research was providing funds to support ADNI clinical sites in Canada. Private sector contributions are facilitated by the Foundation for the National Institutes of Health (www.fnih.org). This grantee organization was the Northern California Institute for Research and Education, and this study was coordinated by the Alzheimer's Therapeutic Research Institute at the University of Southern California. ADNI data are disseminated by the Laboratory for Neuro Imaging at the University of Southern California.

**Funding** This study was supported by Taipei Medical University Hospital, with grants numbered 105TMU-TMUH-05, 106TMU-TMUH-21, and 107TMU-TMUH-09, along with a grant number TMU110-F-011 from Taipei Medical University. Additionally, funding was provided by the Ministry of Science and Technology, Republic of China, under grant number MOST108-2221-E-038–007-MY2.

**Data availability** The datasets presented in this study are available in the Alzheimer's Disease Neuroimaging Initiative (ADNI) repository, https://adni.loni.usc.edu/.

## Declarations

**Conflicts of interest/Competing interests** We declare that we have no conflict of interest. Hui-Hsien Lin worked for Rotary Trading Co., Ltd. The other authors confirmed that the study was carried out without any affiliations or financial ties that could be seen as a possible conflict of interest and that Rotary Trading Co., Ltd did not participate in analysis or writing of this manuscript.

**Ethics approval** All procedures performed in the ADNI studies involving human participants were in accordance with the ethical standards of the institutional research committees and with the 1964 Helsinki declaration and its later amendments.

**Informed consent** Written informed consent was obtained from all participants or their authorized representatives. The study procedures were approved by the institutional review boards of all participating sites and more details can be found at: (http://adni.loni.usc.edu/wp-content/uploads/how_to_apply/ADNI_Acknowledgement_List.pdf).

## References

1. Lin SY, Lin PC, Lin YC et al (2022) The Clinical Course of Early and Late Mild Cognitive Impairment. Front Neurol 13:685636
2. Morris JC, Storandt M, Miller JP et al (2001) Mild cognitive impairment represents early-stage Alzheimer disease. Arch Neurol 58:397–405
3. Jessen F, Wolfsgruber S, Wiese B et al (2014) AD dementia risk in late MCI, in early MCI, and in subjective memory impairment. Alzheimers Dement 10:76–83
4. Aisen PS, Petersen RC, Donohue MC et al (2010) Clinical Core of the Alzheimer's Disease Neuroimaging Initiative: progress and plans. Alzheimers Dement 6:239–246
5. Cai S, Huang L, Zou J et al (2015) Changes in thalamic connectivity in the early and late stages of amnestic mild cognitive impairment: a resting-state functional magnetic resonance study from ADNI. PLoS ONE 10:e0115573
6. Weiner MW, Veitch DP, Aisen PS et al (2015) 2014 Update of the Alzheimer's Disease Neuroimaging Initiative: A review of papers published since its inception. Alzheimer's Dementia 11:e1-120
7. Jessen F, Wolfsgruber S, Wiese B et al (2014) AD dementia risk in late MCI, in early MCI, and in subjective memory impairment. Alzheimer's Dementia 10:76–83
8. Edmonds EC, McDonald CR, Marshall A et al (2019) Early versus late MCI: Improved MCI staging using a neuropsychological approach. Alzheimer's Dementia 15:699–708
9. Jitsuishi T, Yamaguchi A (2022) Searching for optimal machine learning model to classify mild cognitive impairment (MCI) subtypes using multimodal MRI data. Sci Rep 12:4284
10. Zamani J, Sadr A, Javadi AH (2022) Classification of early-MCI patients from healthy controls using evolutionary optimization of graph measures of resting-state fMRI, for the Alzheimer's disease neuroimaging initiative. PLoS ONE 17:e0267608
11. Mesulam MM (2013) Cholinergic circuitry of the human nucleus basalis and its fate in Alzheimer's disease. J Comparative Neurol 521:4124–4144
12. Schmitz TW, Mur M, Aghourian M, Bedard M-A, Spreng RN (2018) Longitudinal Alzheimer's Degeneration Reflects the

Spatial Topography of Cholinergic Basal Forebrain Projections. Cell Rep 24:38–46
13. Arendt T, Brückner MK, Morawski M, Jäger C, Gertz H-J (2015) Early neurone loss in Alzheimer's disease: cortical or subcortical? Acta Neuropathol Commun 3:1–11
14. Baker-Nigh A, Vahedi S, Davis EG et al (2015) Neuronal amyloid-β accumulation within cholinergic basal forebrain in ageing and Alzheimer's disease. Brain 138:1722–1737
15. Braak H, Del Tredici K (2015) The preclinical phase of the pathological process underlying sporadic Alzheimer's disease. Brain 138:2814–2833
16. Schmitz T, Nathan Spreng R (2016) Alzheimer's Disease Neuroimaging I (2016) Basal forebrain degeneration precedes and predicts the cortical spread of Alzheimer's pathology. Nat Commun 7:13249
17. Kondo H, Zaborszky L (2016) Topographic organization of the basal forebrain projections to the perirhinal, postrhinal, and entorhinal cortex in rats. J Comparative Neurol 524:2503–2515
18. Fernández-Cabello S, Kronbichler M, Van Dijk KRA et al (2020) Basal forebrain volume reliably predicts the cortical spread of Alzheimer's degeneration. Brain 143:993–1009
19. Castellano JM, Kim J, Stewart FR et al (2011) Human apoE Isoforms Differentially Regulate Brain Amyloid-β Peptide Clearance. Sci Translat Med 3:89ra57-89ra57
20. Chai AB, Lam HHJ, Kockx M, Gelissen IC (2021) Apolipoprotein E isoform-dependent effects on the processing of Alzheimer's amyloid-β. Biochimica et Biophysica Acta (BBA) - Molecular and Cell Biology of Lipids 1866:158980 https://doi.org/10.1016/j.bbalip.2021.158980
21. Chen Z-R, Huang J-B, Yang S-L, Hong F-F (2022) Role of Cholinergic Signaling in Alzheimer & Disease. Molecules 27:1816
22. Ramos-Rodriguez JJ, Pacheco-Herrero M, Thyssen D et al (2013) Rapid β-Amyloid Deposition and Cognitive Impairment After Cholinergic Denervation in APP/PS1 Mice. J Neuropathol Exp Neurol 72:272–285
23. Hampel H, Mesulam M-M, Cuello AC et al (2018) The cholinergic system in the pathophysiology and treatment of Alzheimer's disease. Brain 141:1917–1933
24. Hoskin JL, Al-Hasan Y, Sabbagh MN (2018) Nicotinic Acetylcholine Receptor Agonists for the Treatment of Alzheimer's Dementia: An Update. Nicotine Tob Res 21:370–376
25. Bott JB, Héraud C, Cosquer B et al (2016) APOE-Sensitive Cholinergic Sprouting Compensates for Hippocampal Dysfunctions Due to Reduced Entorhinal Input. J Neurosci 36:10472–10486
26. Weiner MW, Veitch DP, Aisen PS et al (2012) The Alzheimer's Disease Neuroimaging Initiative: a review of papers published since its inception. Alzheimer's Dementia 8:S1–S68
27. Crane PK, Carle A, Gibbons LE et al (2012) Development and assessment of a composite score for memory in the Alzheimer's Disease Neuroimaging Initiative (ADNI). Brain Imaging Behav 6:502–516
28. Gibbons LE, Carle AC, Mackin RS et al (2012) A composite score for executive functioning, validated in Alzheimer's Disease Neuroimaging Initiative (ADNI) participants with baseline mild cognitive impairment. Brain Imaging Behav 6:517–527
29. Eickhoff SB, Stephan KE, Mohlberg H et al (2005) A new SPM toolbox for combining probabilistic cytoarchitectonic maps and functional imaging data. Neuroimage 25:1325–1335
30. Anthoula T, Marianna S, Penelope M et al (2018) Co morbidity and neuroimaging in Alzheimer's. Gerontology & Geriatrics Studies. https://scholar.google.com.tw/scholar?hl=zh-TW&as_sdt=0%2C5&q=Anthoula+T%2C+Marianna+S%2C+Penelope+M+et+al+%282018%29+Co+morbidity+and+Neuroimaging+in+Alzheimer%E2%80%99s.+Gerontology+%26+Geriatrics+Studies
31. Zaborszky L, Hoemke L, Mohlberg H, Schleicher A, Amunts K, Zilles K (2008) Stereotaxic probabilistic maps of the magnocellular cell groups in human basal forebrain. Neuroimage 42:1127–1141
32. Gaser C, Kurth F (2017) Manual computational anatomy toolbox-CAT12. University of Jena, Structural brain mapping Group at the Departments of Psychiatry and Neurology
33. Nemoto K, Dan I, Rorden C et al (2011) Lin4Neuro: a customized Linux distribution ready for neuroimaging analysis. BMC Med Imaging 11:3–3
34. Núñez C, Callén A, Lombardini F, Compta Y, Stephan-Otto C, AsDN I (2020) Different cortical gyrification patterns in Alzheimer's disease and impact on memory performance. Ann Neurol 88:67–80
35. Gaser C, Dahnke R, Thompson PM, Kurth F, Luders E, Initiative AsDN (2022) CAT – A Computational Anatomy Toolbox for the Analysis of Structural MRI Data. bioRxiv. https://doi.org/10.1101/2022.06.11.495736:2022.2006.2011.495736
36. Smith SM, Nichols TE (2009) Threshold-free cluster enhancement: addressing problems of smoothing, threshold dependence and localisation in cluster inference. Neuroimage 44:83–98
37. Cortes C, Vapnik V (1995) Support-vector networks Machine learning 20:273–297
38. Camps-Valls G, Gómez-Chova L, Calpe-Maravilla J et al (2004) Robust support vector method for hyperspectral data classification and knowledge discovery. IEEE Trans Geosci Remote Sens 42:1530–1542
39. Guo S, Lai C, Wu C et al (2017) Conversion discriminative analysis on mild cognitive impairment using multiple cortical features from MR images. Front Aging Neurosci 9:146
40. Bisong E (2019) Building machine learning and deep learning models on Google cloud platform. Springer
41. Paper (2020) Hands-on Scikit-Learn for Machine Learning Applications. Apress https://doi.org/10.1007/978-1-4842-5373-1
42. Garreta R, Moncecchi G (2013) Learning scikit-learn: machine learning in python. Packt Publishing Ltd. https://scholar.google.com.tw/scholar?hl=zh-TW&as_sdt=0%2C5&q=Garreta+R%2C+Moncecchi+G+%282013%29+Learning+scikit-learn%3A+machine+learning+in+python.+Packt+Publishing+Ltd&btnG=
43. DeLong ER, DeLong DM, Clarke-Pearson DL (1988) Comparing the areas under two or more correlated receiver operating characteristic curves: a nonparametric approach. Biometrics 44:837–845
44. Bachli MB, Sedeño L, Ochab JK et al (2020) Evaluating the reliability of neurocognitive biomarkers of neurodegenerative diseases across countries: A machine learning approach. Neuroimage 208:116456
45. Liu Y, Tan L, Wang H-F et al (2016) Multiple effect of APOE genotype on clinical and neuroimaging biomarkers across Alzheimer's disease spectrum. Mol Neurobiol 53:4539–4547
46. Jack CR Jr, Knopman DS, Jagust WJ et al (2010) Hypothetical model of dynamic biomarkers of the Alzheimer's pathological cascade. The Lancet Neurology 9:119–128
47. Lim YY, Laws SM, Villemagne VL et al (2016) Aβ-related memory decline in APOE ε4 noncarriers: Implications for Alzheimer disease. Neurology 86:1635–1642
48. Bekdash RA (2021) The Cholinergic System, the Adrenergic System and the Neuropathology of Alzheimer's Disease. Int J Mol Sci 22:1273
49. Schmitz TW, Soreq H, Poirier J, Spreng RN (2020) Longitudinal basal forebrain degeneration interacts with trem2/c3 biomarkers of inflammation in presymptomatic Alzheimer's disease. J Neurosci 40:1931–1942
50. La Joie R, Bejanin A, Fagan AM et al (2018) Associations between [18F] AV1451 tau PET and CSF measures of tau pathology in a clinical sample. Neurology 90:e282–e290

51. Suzuki K, Hirakawa A, Ihara R et al (2020) Effect of apolipoprotein E ε4 allele on the progression of cognitive decline in the early stage of Alzheimer's disease. Alzheimer's Dementia: Translat Res Clin Interventions 6:e12007
52. O'Donoghue MC, Murphy SE, Zamboni G, Nobre AC, Mackay CE (2018) APOE genotype and cognition in healthy individuals at risk of Alzheimer's disease: A review. Cortex 104:103–123



## Authors and Affiliations

**Ying-Liang Larry Lai[1] · Fei-Ting Hsu[2] · Shu-Yi Yeh[3] · Yu-Tzu Kuo[3] · Hui-Hsien Lin[4] · Yi-Chun Lin[3] · Li-Wei Kuo[5,6] · Cheng-Yu Chen[7,8] · Hua-Shan Liu[3,9] · for the Alzheimer's Disease Neuroimaging Initiative**

✉ Cheng-Yu Chen
sandy0932@gmail.com

✉ Hua-Shan Liu
HeatherLiu2016@gmail.com

[1] Ph.D. Program in Medical Neuroscience, College of Medical Science and Technology, Taipei Medical University and National Health Research Institutes, Taipei, Taiwan

[2] Department of Biological Science and Technology, China Medical University, Taichung, Taiwan

[3] School of Biomedical Engineering, College of Biomedical Engineering, Taipei Medical University, Taipei, Taiwan

[4] CT/MR Division, Rotary Trading CO., LTD, Taipei, Taiwan

[5] Institute of Biomedical Engineering and Nanomedicine, National Health Research Institutes, Miaoli, Taiwan

[6] Institute of Medical Device and Imaging, National Taiwan University College of Medicine, Taipei, Taiwan

[7] Department of Radiology, School of Medicine, College of Medicine, Taipei Medical University, Taipei, Taiwan

[8] Department of Medical Imaging, Taipei Medical University Hospital, Medical University, Taipei, Taiwan

[9] International Ph.D. Program in Biomedical Engineering, College of Biomedical Engineering, Taipei Medical University, Taipei, Taiwan